

# **9Th Semester Project**

**Field dependence of spin wave dispersion of splay phase of the  
ferromagnetic pyrochlore lattice**

*Submitted*

*by*

**Haraprasad Dhal**

*Guided*

*by*

**Dr. V. Ravi Chandra**



**School of Physical Sciences**

**National Institute of Science Education and Research**

**Bhubaneswar**

**Date :November 27, 2022**

## **ACKNOWLEDGEMENTS**

I wish to thank Dr. V. Ravi Chandra for giving me the opportunity to work with him and guiding me for my 9Th Semester project work.I also wish to Thank V.V Jyothis for his suggestions and guidance.

## **ABSTRACT**

We have applied spin wave theory to ferromagnetic Pyrochlore Lattice with exchange interaction,Dzyaloshinsky-Moriya interaction(DMI),single site anisotropy and presence of a static external magnetic field.In this semester We have generated spin wave spectrum data for different values of interaction strengths and magnetic field strength as well its direction. For this report we have presented the data for a fixed value of interaction strengths.The spin wave dispersion relation are found to have weyl points.We also found that as we change the magnetic field,the spectra changes and the position weyl points vary.The motivation is that:As presented in Onose et al[8],Direction of field has no influence on thermal hall effect ,Where as calculation by V.V Jyothis et. al.[3] for slab geometries show that,magnonic dispersion depends on direction of truncation for building the slabs.So We are intrested in calculation of thermal hall effects,for which magnon spectra calculation and Berry curvature calculation are key ingredients.

# Contents

<b>1</b>	<b>Introduction</b>	<b>1</b>
<b>2</b>	<b>Magnon Spectrum Calculation</b>	<b>4</b>
2.1	Zero Magnetic field Spectrum: . . . . .	6
2.2	Non zero Magnetic field Spectrum . . . . .	7
2.2.1	Field direction along [100]: . . . . .	7
2.2.2	Field direction along [110]: . . . . .	7
2.2.3	Field Direction along [111]: . . . . .	9
2.3	Field Rotation . . . . .	11
2.3.1	Field Direction Rotation: [100] → [110] . . . . .	12
2.3.2	Field Direction Rotation: [111] → [100] . . . . .	16
2.3.3	Field Direction Rotation: [111] → [110] . . . . .	18
<b>3</b>	<b>Summary and Conclusions</b>	<b>21</b>
<b>Appendices</b>		<b>23</b>
<b>Appendix A</b>		<b>23</b>
A.1	Vanishing Linear terms in Local coordinates: . . . . .	23
A.2	High symmetry paths: . . . . .	24
A.3	Python Codes: . . . . .	24

# Chapter 1

## Introduction

We study the ferromagnetic spin system on pyrochlore lattice. The pyrochlore lattice is a sixfold-coordinated structure whose underlying Bravais lattice is FCC, with four basis. The primitive vectors are:  $\{(\frac{1}{2}, \frac{1}{2}, 0), (0, \frac{1}{2}, \frac{1}{2}), (\frac{1}{2}, \frac{1}{2}, 0)\}$ .

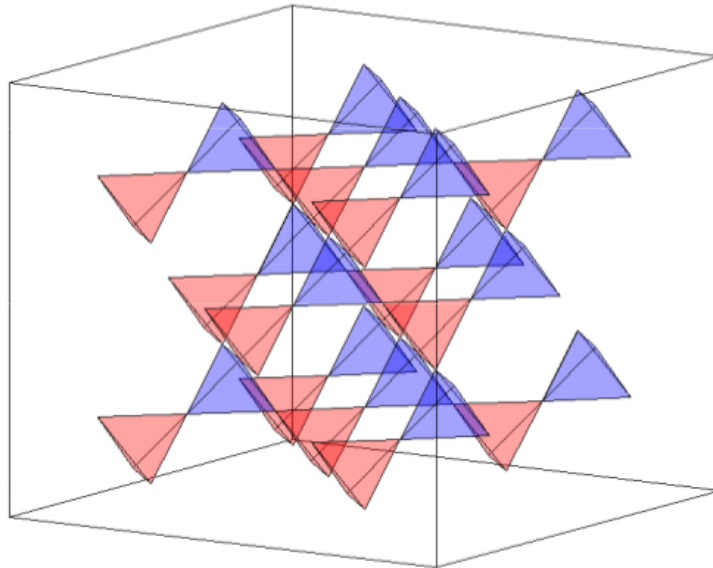


Figure 1.1: Pyrochlore Lattice

We work with following spin Hamiltonian on pyrochlore lattice.

$$H = \sum_{\langle i\alpha, j\beta \rangle} JS_{i\alpha} \cdot S_{j\beta} + \sum_{\langle i\alpha, j\beta \rangle} \mathbf{D}_{i\alpha, j\beta} \cdot \mathbf{S}_{i\alpha} \times \mathbf{S}_{j\beta} + K \sum_{i\alpha} (\mathbf{S}_{i\alpha} \cdot \hat{\mathbf{n}}_\alpha)^2 - \sum_{i\alpha} \mathbf{S}_{i\alpha} \cdot \mathbf{B} \quad (1.1)$$

The First three terms are nearest neighbor Heisenberg exchange, Dzyalonski-moriya interaction(DMI) and the single-site anisotropy respectively. The last term is due to interaction of spins with applied magnetic field  $\mathbf{B}$ .  $\mathbf{S}_{i\alpha}$  are spin  $S$  vector operators at  $\mathbf{R}_{i\alpha} = \mathbf{R}_i + \alpha$  where  $\mathbf{R}_i$  is a Bravais lattice vector of FCC lattice.  $\alpha$  denotes the four sub lattice vectors corresponding to the vertices of tetrahedron,  $\alpha \in [(0, 0, 0), (\frac{1}{4}, \frac{1}{4}, 0), (0, \frac{1}{4}, \frac{1}{4}), (\frac{1}{4}, 0, \frac{1}{4})]$ .  $\mathbf{D}_{i\alpha, j\beta}$  are DMI vectors. We follow the convention

that DMI term for first two sublattices is  $(\frac{-D}{\sqrt{2}}, \frac{D}{\sqrt{2}}, 0) \cdot (\mathbf{S}_{i1} \times \mathbf{S}_{i2})$ . The rest of the vectors are determined by lattice symmetry. We assume  $\mathbf{D}_{i\alpha,j\beta}$  has translation invariance. The local anisotropy axis unit vector for each spin,  $\hat{\mathbf{n}}_\alpha$ , points from the site to the centre of the tetrahedron. We take  $J=-1, D=0.3$  and  $K=-0.3$ . We follow the detailed formalism given in Paper by V.V Jyothis et al.[3] to handle the spin wave Hamiltonian. There they have described it for zero magnetic field ,in this project We modify it to accommodate non zero magnetic field.

The approach mentioned there[3] is to rewrite the Hamiltonian in terms of local spherical coordinates of sub lattices,  $\mathbf{e}_\alpha^m$  ,  $(\mathbf{e}_\alpha^1, \mathbf{e}_\alpha^2, \mathbf{e}_\alpha^3)=(\theta_\alpha, \phi_\alpha, r_\alpha)$ , assuming that the spin configuration have translation invariance. The  $e_\alpha^3$  points along the classical spin direction. When we do the Holstein Primakoff(HP) transformation and carry out the linear spin wave theory(spin excitations<<total spin at sub lattice sites),the coefficients of linear terms vanish in this local coordinates. We will be left with a Hamiltonian with only zeroth order terms and second order terms ,which will be bilinear in terms of HP bosonic operators. We drop the higher order terms. It is then possible to diagonalize this form of hamiltonian i.e the bogoliubov transformation. Meanwhile, the difficulty gets transferred to finding the correct classical ground state since there are many extreums in the landscape of Hamiltonian as a function of classical spin configuration .Working with incorrect ground state configuration may lead to failure of the diagonalization. The classical Ground state for ferromagnetic pyrochlore with the Hamiltonian of the form above without the external magnetic field, is known to be ferromagnetic splay state from Luttinger Tisza [5] method. The moments in tetrahedron have following moments in x direction splay phase: $\{(a,b,b),(a,b,-b),(a,-b,-b),(a,-b,b)\}$ . But it works only in zero field. To find the same for non zero field We apply minimization to the Hamiltonian starting with the guess value for the minimization algorithm same as the result from Luttinger-Tisza method. As we increase the field strength slowly we take the guess value for the minimization algorithm as the

result of previous field strength. At every step we check that the hessian of the result is positive definite by checking if cholesky decomposition is possible for the result. We also make sure that the linear terms are vanishing by checking it for every time we increase the field strength. In the next chapter we describe the form the Hamiltonian takes in local coordinate. We then do the Fourier transformation following HP Bosonic transformation. We Diagoanlize and plot the spectrum for different field strengths and direction.

# Chapter 2

## Magnon Spectrum Calculation

We write the Hamiltonian in Local spin coordinates and represent it in terms of spin ladder operators.

$$S_{i\alpha}^+ = S_{i\alpha}^1 + iS_{i\alpha}^2 = (S_{i\alpha}^-)^\dagger$$

$$\begin{aligned} \mathbf{H} = & \sum_{i\alpha,j\beta} [J_{i\alpha;j\beta}^{33} S_{i\alpha}^3 S_{j\beta}^3 + J_{i\alpha;j\beta}^{++} S_{i\alpha}^+ S_{j\beta}^+ + J_{i\alpha;j\beta}^{--} S_{i\alpha}^- S_{j\beta}^- + J_{i\alpha;j\beta}^{+-} S_{i\alpha}^+ S_{j\beta}^- + J_{i\alpha;j\beta}^{-+} S_{i\alpha}^- S_{j\beta}^+ \\ & + J_{i\alpha;j\beta}^{+3} S_{i\alpha}^+ S_{j\beta}^3 + J_{i\alpha;j\beta}^{3+} S_{i\alpha}^3 S_{j\beta}^+ + J_{i\alpha;j\beta}^{-3} S_{i\alpha}^- S_{j\beta}^3 + J_{i\alpha;j\beta}^{3-} S_{i\alpha}^3 S_{j\beta}^-] \\ & - \sum_{i\alpha} [\mathcal{B}^3 S_{i\alpha}^3 + \mathcal{B}^+ S_{i\alpha}^+ + \mathcal{B}^- S_{i\alpha}^-] \end{aligned} \quad (2.1)$$

Where these new coefficients that appear in front of spin ladder operators contains all the information about coefficients of exchange interaction ,DMI,spin site anisotropy and magnetic field in terms of local spin coordinate.We have omitted the nearest neighbour symbol  $<>$  in the summation but the coefficients are zero when  $i\alpha$  and  $j\beta$  are not nearest neighbours.

Next, we map the spin ladder operators to Bosonic operators via Holstein-Primakoff transformation. ( $S_{i\alpha}^3 = S - b_{i\alpha}^\dagger b_{i\alpha}$ ,  $S_{i\alpha}^+ = \sqrt{2S - b_{i\alpha}^\dagger b_{i\alpha}} b_{i\alpha}$ ) and keep terms only up to second order.The first order terms are:

$$\sum_{i\alpha} \sqrt{2S} \left[ \sum_{j\beta} S[J_{i\alpha;j\beta}^{+3} + J_{j\beta;i\alpha}^{3+}] - \mathcal{B}^+ \right] b_{i\alpha} = 0 \quad (2.2)$$

$$\sum_{i\alpha} \sqrt{2S} \left[ \sum_{j\beta} S[J_{i\alpha;j\beta}^{-3} + J_{j\beta;i\alpha}^{3-}] - \mathcal{B}^- \right] b_{i\alpha}^\dagger = 0 \quad (2.3)$$

We argue that the coefficients of  $b_{i\alpha}$  vanish for the local axis that we defined previously.Hence first order terms vanish.We derive the result by setting the derivatives of Hamiltonian in equation 2.1 with respect to  $S_{i\alpha}^1$  and  $S_{i\alpha}^2$  to zero in the ground state

configuration. More details are given in appendix A.1. We then express the Hamiltonian in momentum space. The convention for Fourier transformation is as follows

$$\hat{O}_{q\alpha} = \frac{1}{N} \sum_i \hat{O}_{i\alpha} \exp(-i\mathbf{q}\cdot\mathbf{R}_i) \quad (2.4)$$

$$\tilde{T}_{\alpha\beta}(q) = \sum_{\Delta_{\alpha\beta}} T_{i\alpha;j\beta} \exp(-i\mathbf{q}\cdot\Delta_{\alpha\beta}) \quad (2.5)$$

Where  $\Delta_{\alpha\beta}$  is the Bravais lattice vector joining the two sites  $\mathbf{R}_j - \mathbf{R}_i$ . This Fourier transformation is possible assuming  $T$  has translational invariance. Here,  $N = \prod_i N_i$  is the number of Bravais lattice sites and periodic boundary condition is used so that  $q = \sum_i \frac{m_i}{N_i} \mathbf{K}_i$ ,  $m_i \in [0, N_i - 1]$ . The Hamiltonian takes following form.

$$\mathbf{H} = \varepsilon_0 + \sum'_{\mathbf{q}} \begin{bmatrix} (\mathbf{b}_{\mathbf{q}}^\dagger)^T & (\mathbf{b}_{-\mathbf{q}})^T \end{bmatrix} \begin{bmatrix} \mathcal{A}_q & \mathcal{C}_q \\ \mathcal{C}_q^\dagger & \mathcal{A}_{-q}^T \end{bmatrix} \begin{bmatrix} \mathbf{b}_{\mathbf{q}} \\ \mathbf{b}_{-\mathbf{q}}^\dagger \end{bmatrix} \quad (2.6)$$

Where,

$$\begin{aligned} \varepsilon_0 &= NS(S+1) \sum_{\alpha\beta} \tilde{J}_{\alpha\beta}^{33}(0) + 2S \sum'_{\mathbf{q}\alpha} \eta_{\mathbf{q}} [\tilde{J}_{\alpha\alpha}^{+-}(\mathbf{q}) - \tilde{J}_{\alpha\alpha}^{-+}(\mathbf{q})] + \sum_{\mathbf{q}\alpha} \mathcal{B}_\alpha^3 \\ [\mathcal{A}_{\mathbf{q}}]_{\alpha\beta} &= -\eta_{\mathbf{q}} \left[ S \sum_{\beta'} [\tilde{J}_{\alpha\beta'}^{33}(0) + \tilde{J}_{\beta'\alpha}^{33}(0)] + \mathcal{B}_\alpha^3 \right] \delta_{\alpha\beta} + 2S\eta_{\mathbf{q}} [\tilde{J}_{\beta\alpha}^{+-}(\mathbf{q}) - \tilde{J}_{\alpha\beta}^{+-}(-\mathbf{q})] \\ [\mathcal{C}]_{\alpha\beta} &= 2S\eta_{\mathbf{q}} [\tilde{J}_{\alpha\beta}^{--}(-\mathbf{q}) - \tilde{J}_{\beta\alpha}^{--}(\mathbf{q})] \end{aligned} \quad (2.7)$$

The matrix in equation 1.17 is of order  $2 \times n_s$  where  $n_s$  is number of sublattice sites.  $\mathbf{b}_{\mathbf{q}}$  and  $\mathbf{b}_{\mathbf{q}}^\dagger$  are column vectors of  $\{ b_{\mathbf{q}\alpha} \}$  and  $\{ b_{\mathbf{q}\alpha}^\dagger \}$ .  $\sum'$  indicates sum is taken over distinct pairs of  $(\mathbf{q}, -\mathbf{q})$ .  $\eta_{\mathbf{q}}$  is 1/2 for those vectors in Brillouin zone for which  $\mathbf{q}$  and  $-\mathbf{q}$  differ by a reciprocal lattice vector and 1 otherwise.

We then find the Eigenvalue spectrum for magnons. We follow the detailed prescription given in J colpa's paper [2] for diagonalizing the Hamiltonian of equation 2.6. In the absence of magnetic field the splay phase is degenerate in any of x,y or z direction. But as we apply the magnetic field this degeneracy breaks for direction

other than x. We apply the magnetic field along [100],[110],[111] directions of varying strength.Along [111] direction We get a stacking of Triangular and Kagome Lattice planes.Along [100] and [110] direction We get square and rectangular Bravais lattice planes respectively.We also look at how the spectrum varies as we rotate the field direction form  $[100] \rightarrow [110]$ , $[110] \rightarrow [111]$  and  $[100] \rightarrow [111]$ .**The motivation behind this is:**In Onose et al.[8], They have presented Thermal hall effect data for different direction of field and the result was same irrespective of field direction.But in the study by V.V Jyothis et.al.[3] They have found that ,in the absence of field ,the slab geometry spectrum for pyrochlore lattice changes when one changes the surface.Also spectrum being reciprocal or non reciprocal depends on the surface on which lattice is terminated to get the slab geometry.This could have some effect in the thermal hall response.That is why we are interested to know what happens to the spectrum when we change the field direction. We plot the spectra on the high symmetry paths.From now on when ever we will come across a spectra figure ,the details about J,D,K and magnetic field are written on the top of figure.If corresponding spin configuration is provided it is plotted to its immediate right or mentioned if otherwise.If there is a black line vector in spin configuration plot ,it indicates the field direction.Also the color of vectors in spin configuration has no relation to color of bands in the spectra.The points corresponding high symmetry path in Brillouin zone is given in appendix.In comparison to the literature, the G point in this report is same as  $\Gamma$  i.e the origin of Brillouin zone.

## 2.1 Zero Magnetic field Spectrum:

In the absence of magnetic field the lower two bands have degeneracy along X to W path.Upper two bands also have degeneracy between X to W.There is a crossing between band 2 and 3 on the path between G and X.The corresponding  $\mathbf{q}$  point on the Brillouin zone is [2.2619,0,0].

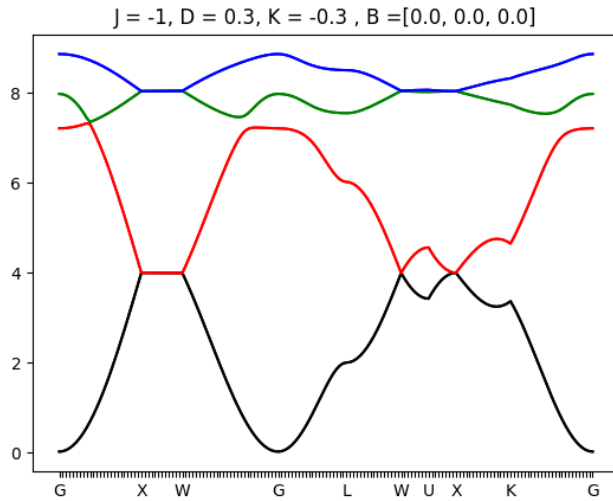


Figure 2.1: zero Magnetic field spin wave Spectrum

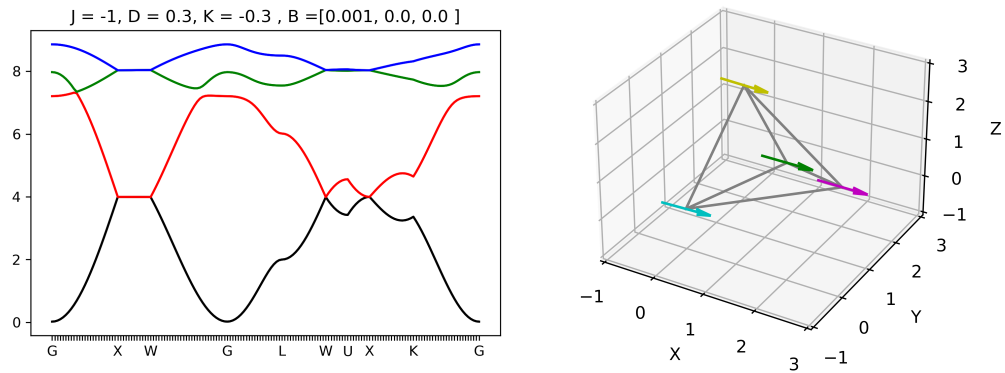
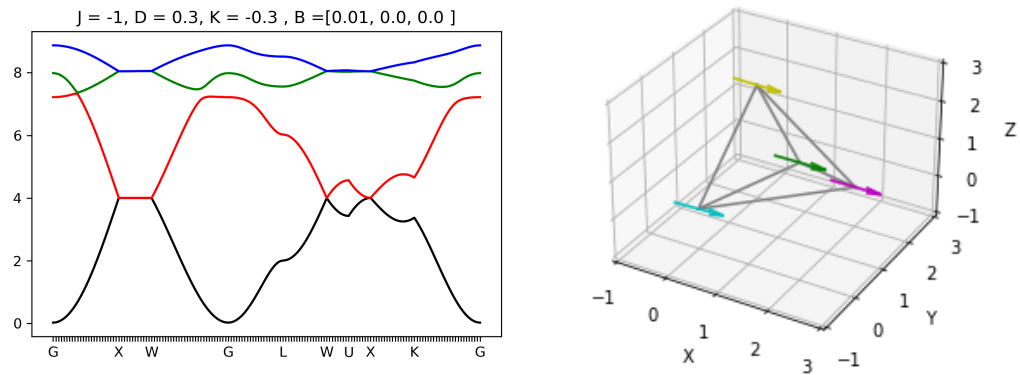
## 2.2 Non zero Magnetic field Spectrum

### 2.2.1 Field direction along [100]:

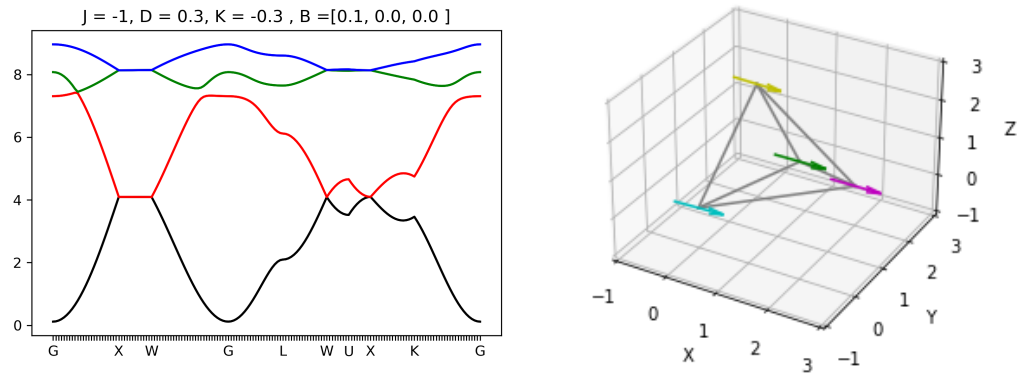
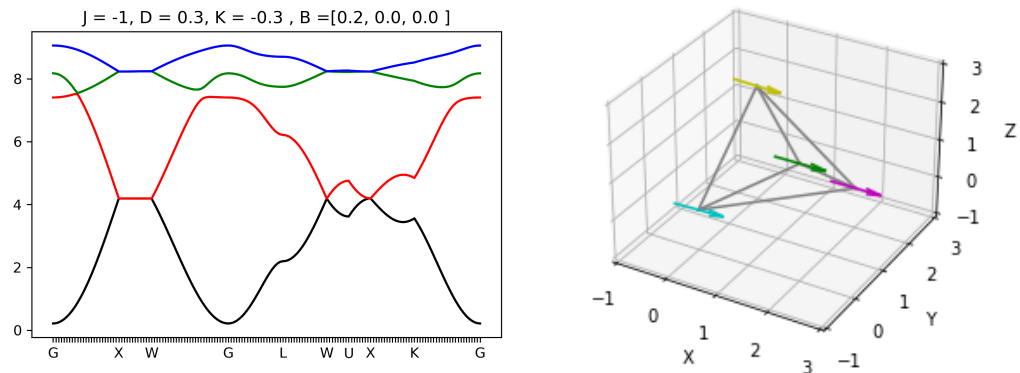
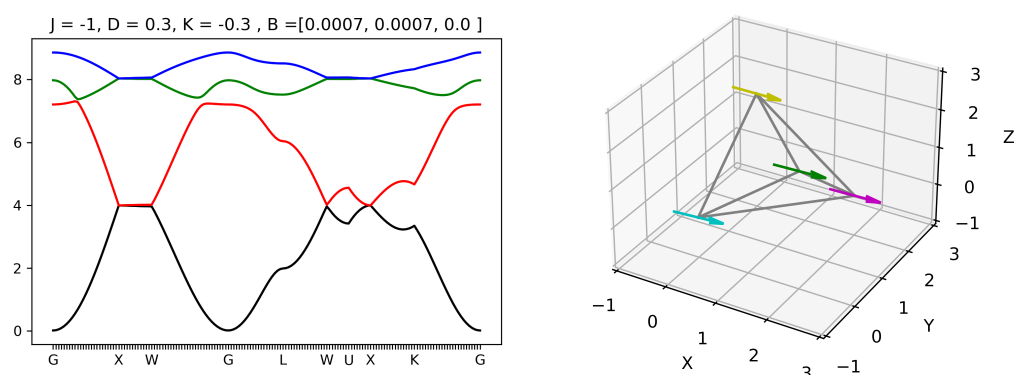
There is almost no change in the spectrum apart from scale and gap at G, when we put the magnetic field along [100] from the zero field spectrum ,figure 2.2 to 2.5. As we increase the magnetic field the splay state along magnetic field is favourable. Since We already had a splay ground state along x and now that magnetic field is also along x there is no change in splay state spin configuration. Therefore the spectra remain identical to Splay state along x in zero field. If we increase the field very large ,much larger than DMI strengths,then it will get to completely ferromagnetic state.

### 2.2.2 Field direction along [110]:

When the field strength is very low ,figure 2.6, it's still a splay state along x. The splay state align along magnetic field as we increase the strength ,figure 2.6 to 2.11. The degeneracy between X and W is lifted.bands separates from each other at W but they maintain the degeneracy (band (1 and 2) and band (3 and 4)at X. A crossing appears between K and G as we increase the strength. For the field strength 0.1 ,the

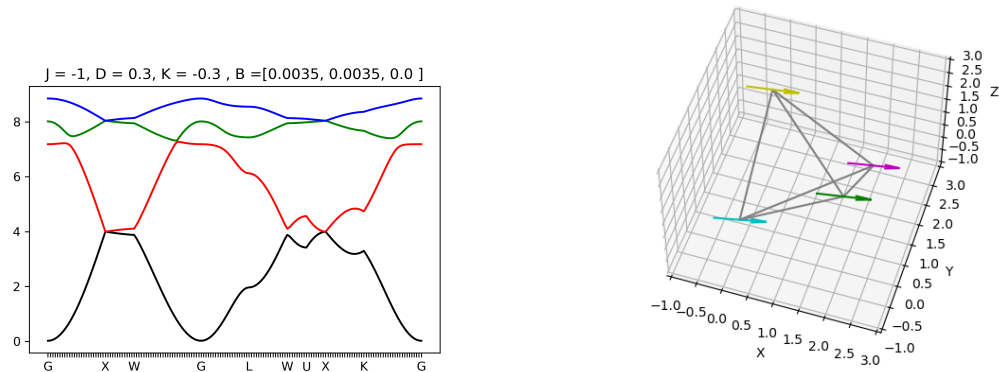
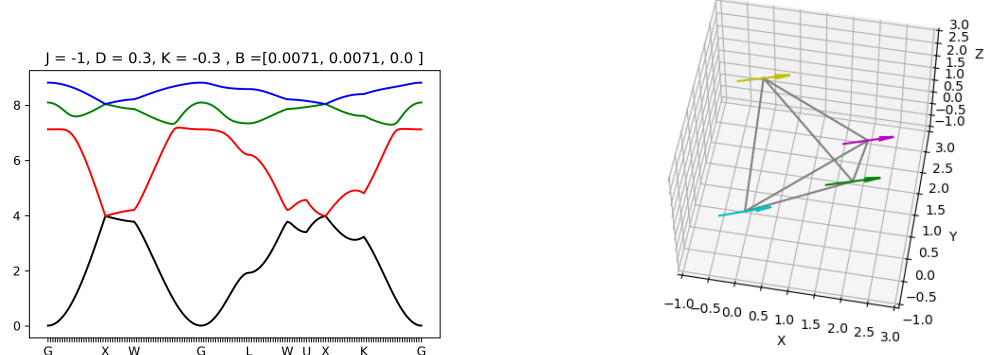

 Figure 2.2:  $B=0.001$ 

 Figure 2.3:  $B=0.01$ 

corresponding  $\mathbf{q}$  value in Brillouin zone is  $[2.2619, 2.1619, 0]$ . Another crossing appears between W and G for  $B=0.005$  but disappears again as we increase the field strength.


 Figure 2.4:  $B=0.1$ 

 Figure 2.5:  $B=0.2$ 

 Figure 2.6:  $B=0.001$ 

### 2.2.3 Field Direction along [111]:

The splay state align along the fields as we increase the strength. Here the bands 1 and 2 separates from each other. Band 3 and 4 also separates from each other, figure 2.12


 Figure 2.7:  $B=0.005$ 

 Figure 2.8:  $B=0.01$ 

to 2.16. The gap between them increases as we increase the field strength. Meanwhile, a crossing point appears between G and L as we increase the field strength. For the field strength of 0.1 the corresponding  $\mathbf{q}$  value in Brillouin zone is [2.2619, 2.2619, 2.2619].

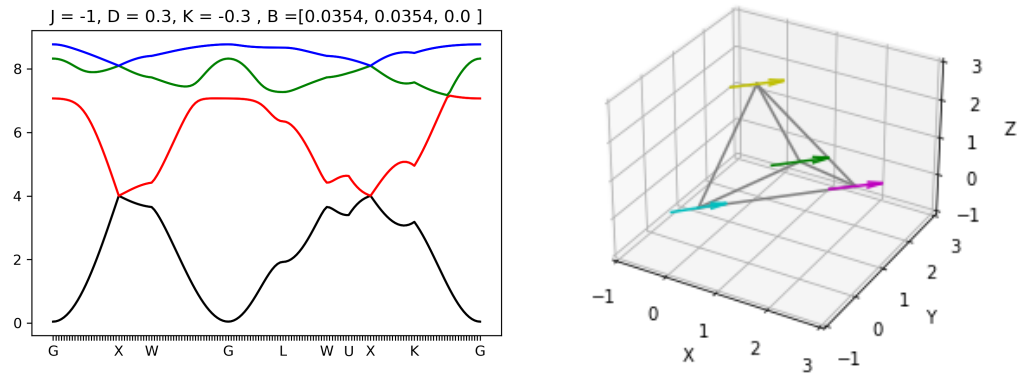


Figure 2.9: B=0.05

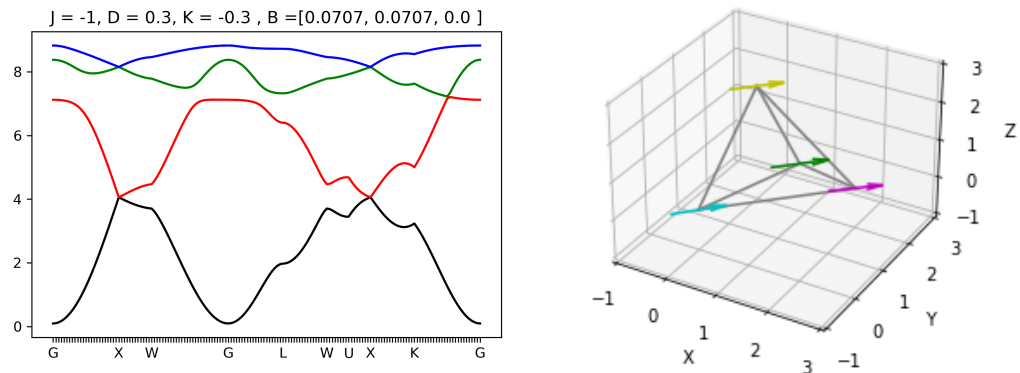


Figure 2.10: B=0.1

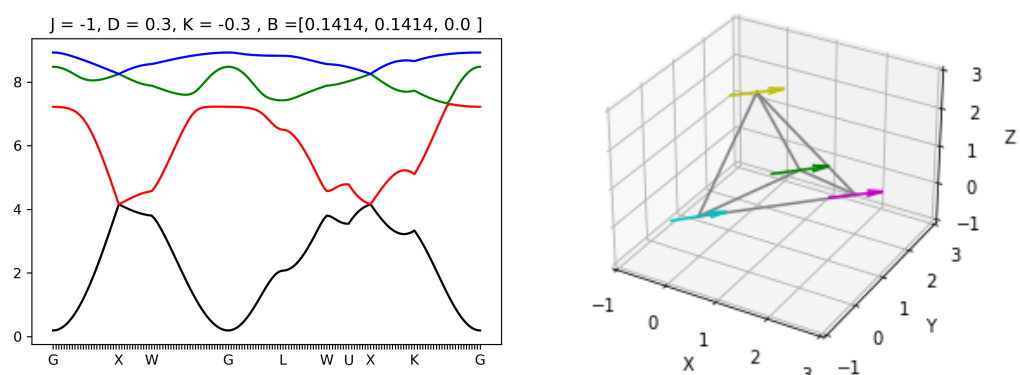
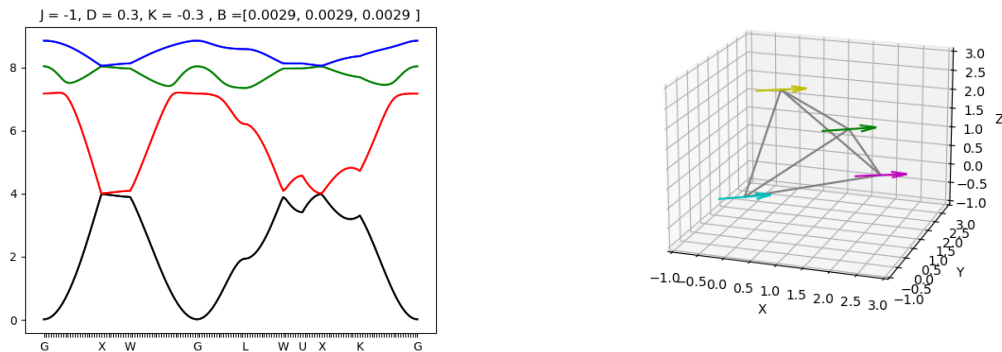
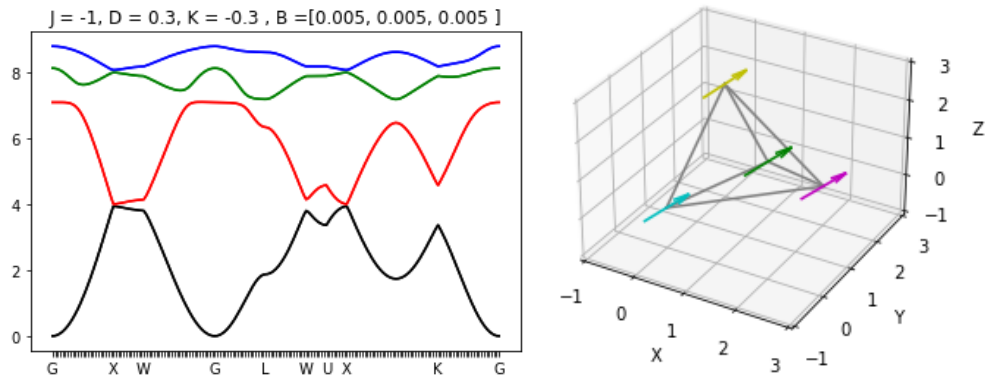


Figure 2.11: B=0.2

## 2.3 Field Rotation

In the previous section We observed that splay state align along magnetic field as we increase the field strength.In this section we will explore what happens to the


 Figure 2.12:  $B=0.005$ 

 Figure 2.13:  $B=0.01$ 

configuration and the spectra as we rotate the field direction, keeping the field strength constant. We keep the constant field strength at  $B=0.1$ .

### 2.3.1 Field Direction Rotation: $[100] \rightarrow [110]$

We rotate the field direction from  $[100]$  to  $[110]$  direction. The splay state configuration rotates with the magnetic field direction as it changes, figure 2.18 to 2.22. The crossing between band 2 and 3 on the path G to X for  $[100]$ , disappears as we change the direction to  $[110]$ . The degeneracy between X and W lifts up. The spectra continuously changes to  $[110]$  direction type with a crossing between same band 2 and 3 on K and G path. Among these transitions, another crossing also appears on W and G

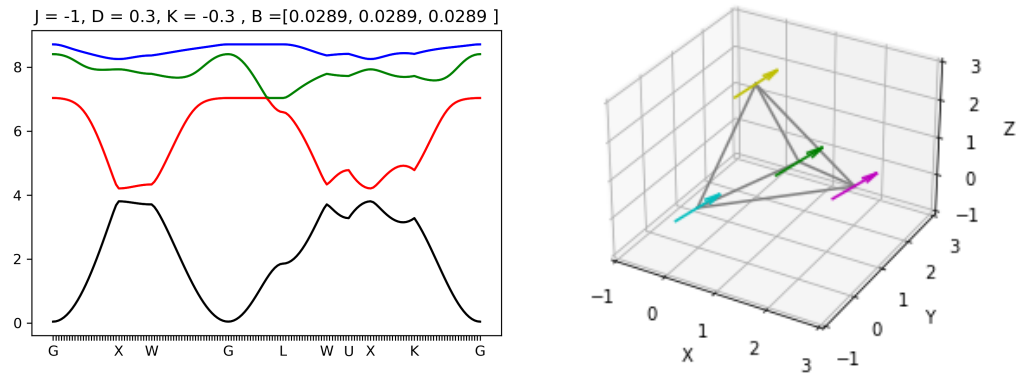


Figure 2.14: B=0.05

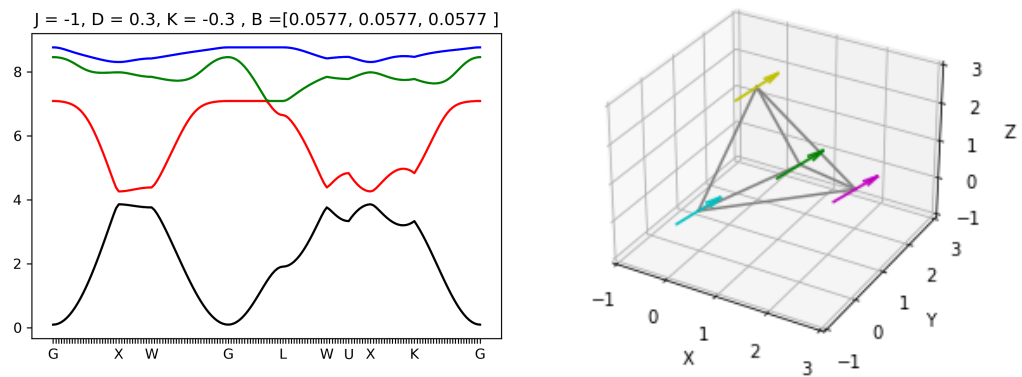


Figure 2.15: B=0.1

path, figure 2.19 , but disappears as the fields direction keeps changing more towards [110].

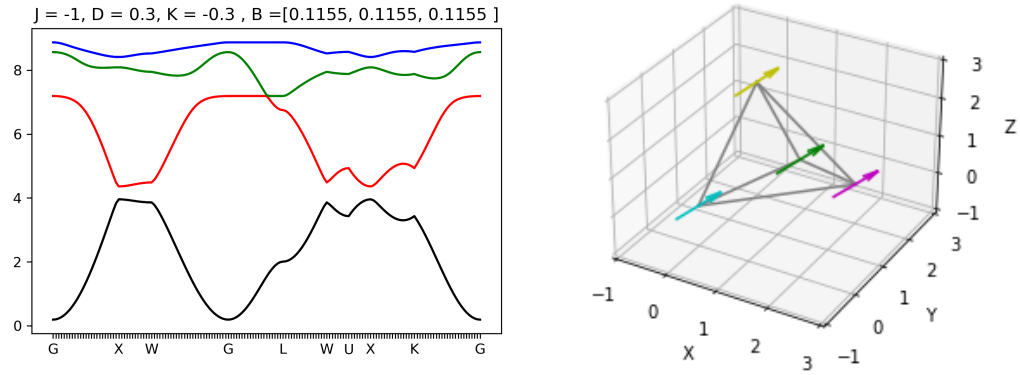


Figure 2.16:  $B=0.2$

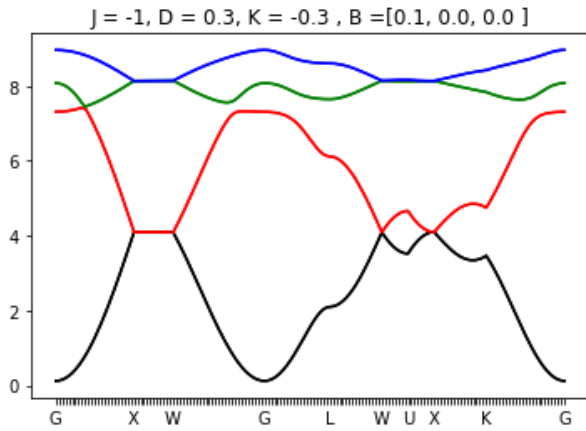


Figure 2.17:

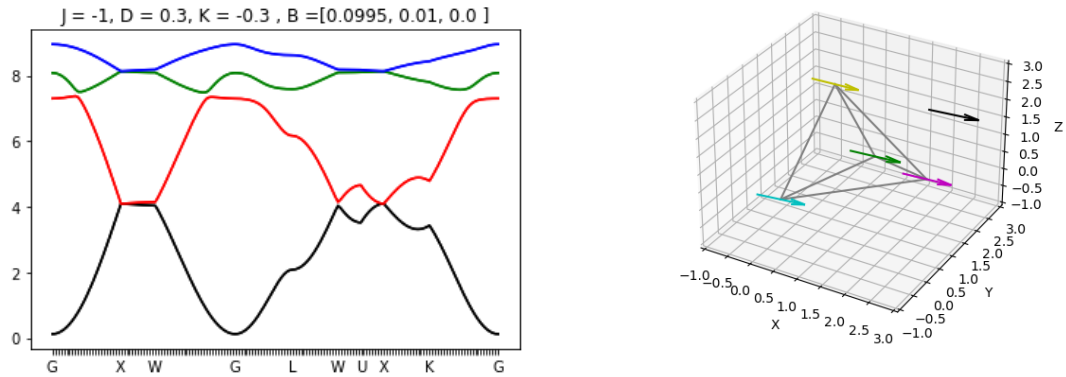


Figure 2.18:

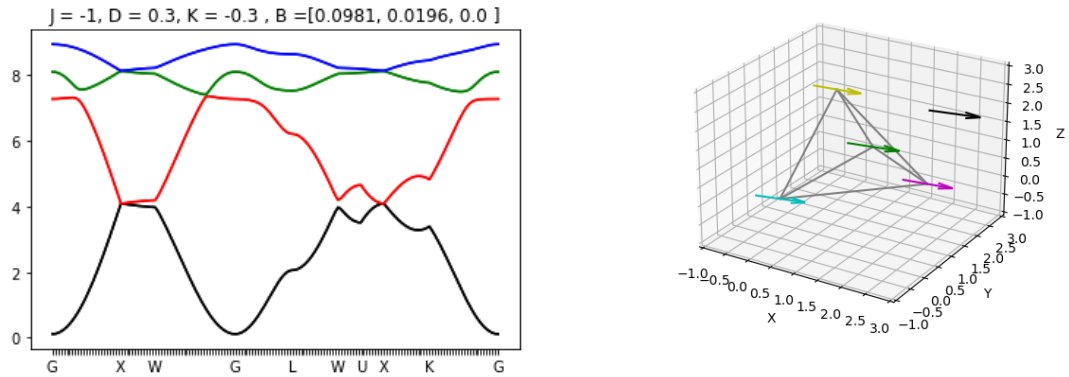


Figure 2.19:

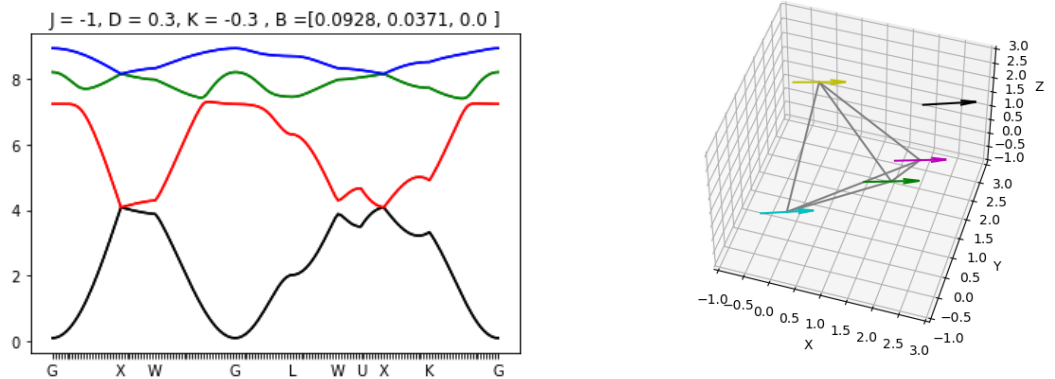


Figure 2.20:

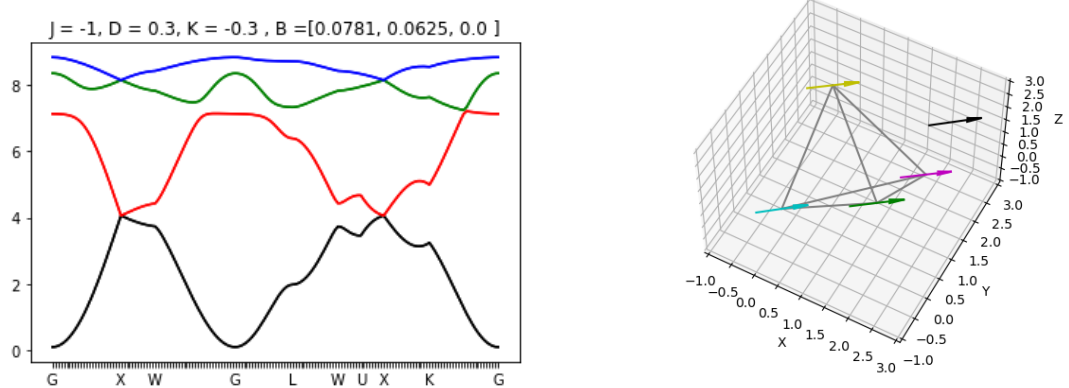


Figure 2.21:

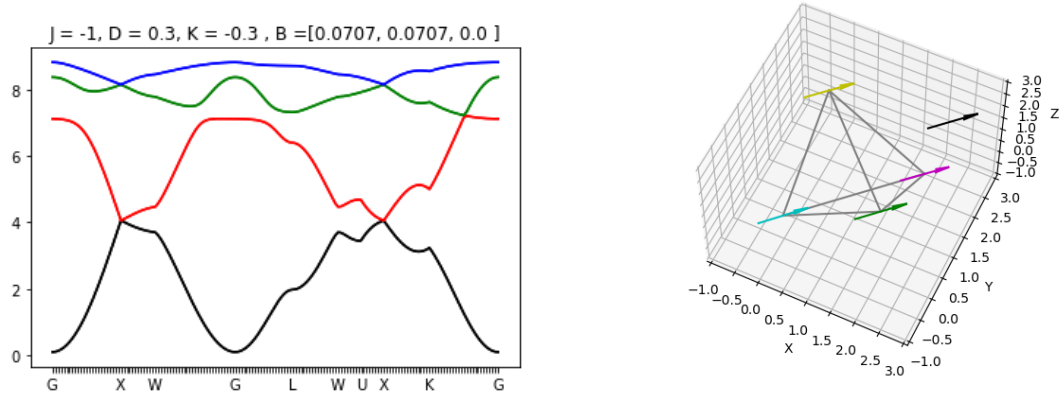


Figure 2.22:

### 2.3.2 Field Direction Rotation: [111] → [100]

As we change the field direction ,the splay state rotates with the field from [111] to [100].The separated Bands start to come closer and the degeneracy between X and W is again established as we reach [100] direction,figure 2.23 to 2.28.The crossing point on the path G and L disappears and appears on G and X as we reach [100].

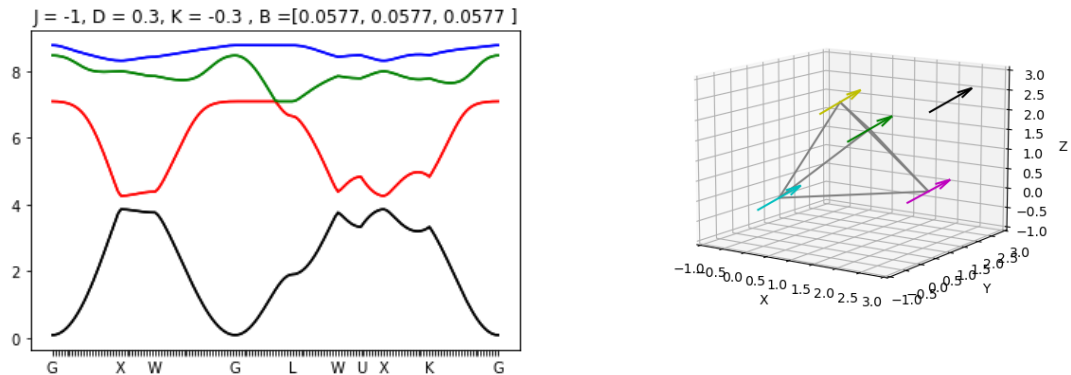


Figure 2.23:

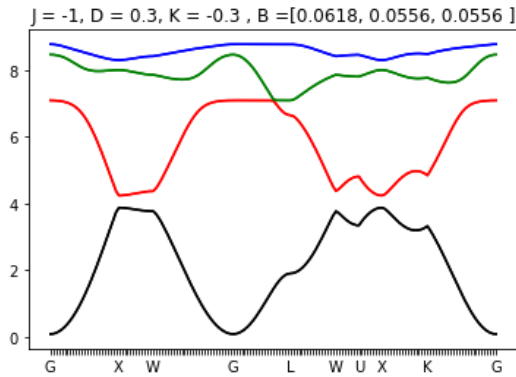


Figure 2.24:

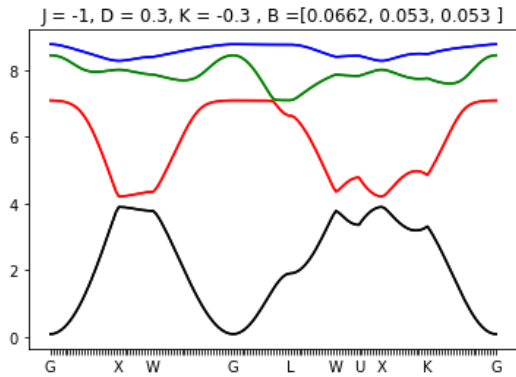


Figure 2.25:

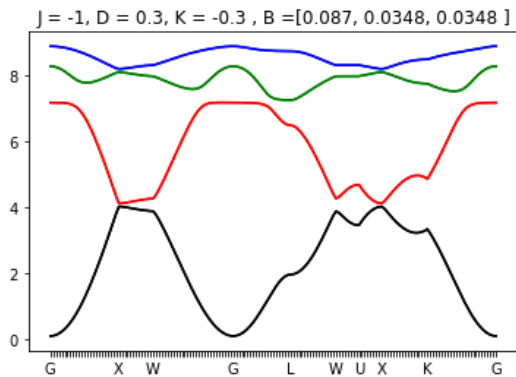


Figure 2.26:

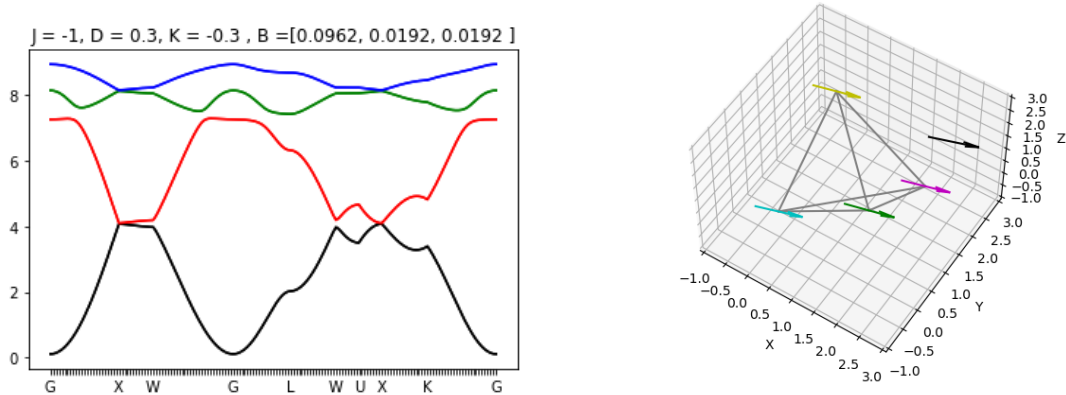


Figure 2.27:

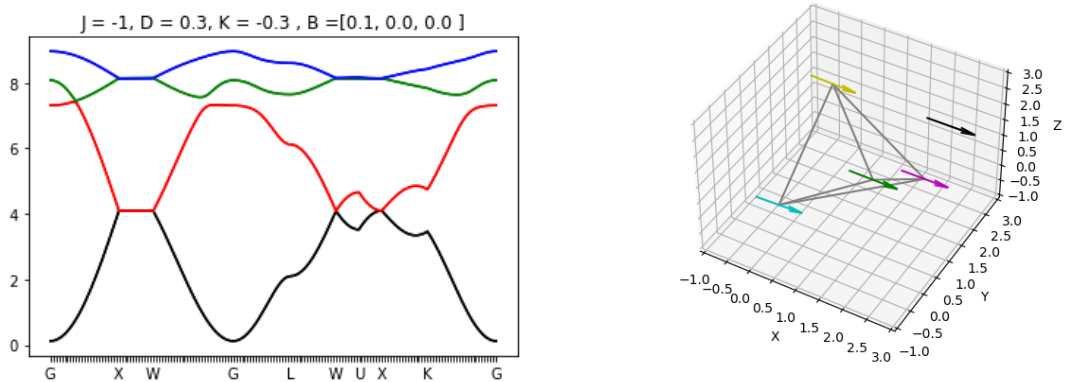


Figure 2.28:

### 2.3.3 Field Direction Rotation:[111]→[110]

We rotate the field from [111] to [110] direction. In [111] direction the bands are completely separated except for the crossing point on the path G and L. As we rotate the field towards [110] the splay state also rotates, aligned with the field direction, figure 2.29 to 2.34. As we get closer to [110] direction a crossing point appears on the path K and G which is characteristic of [110] direction. Finally the spectrum changes completely to [110] type.

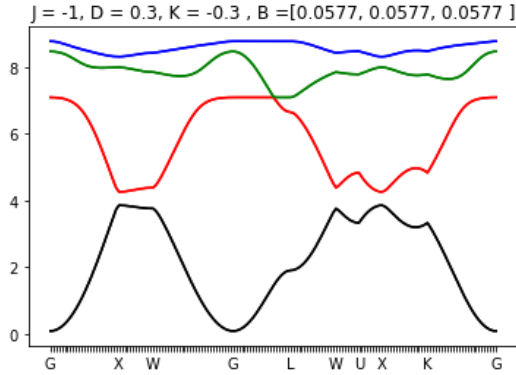


Figure 2.29:

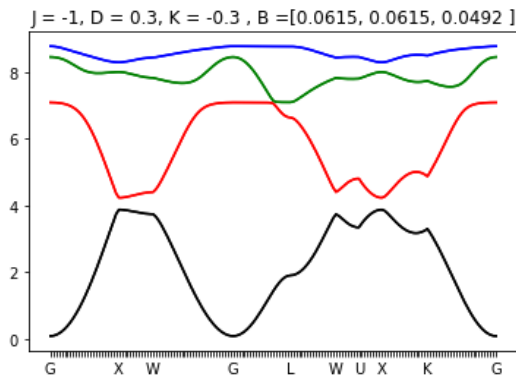


Figure 2.30:

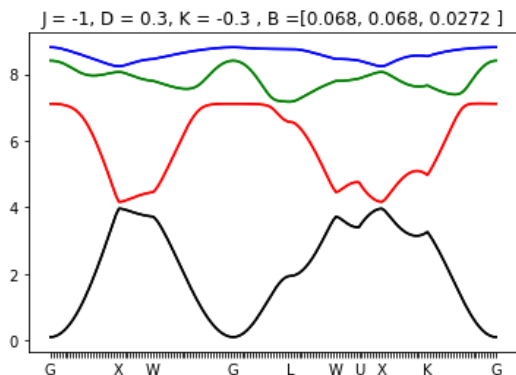


Figure 2.31:

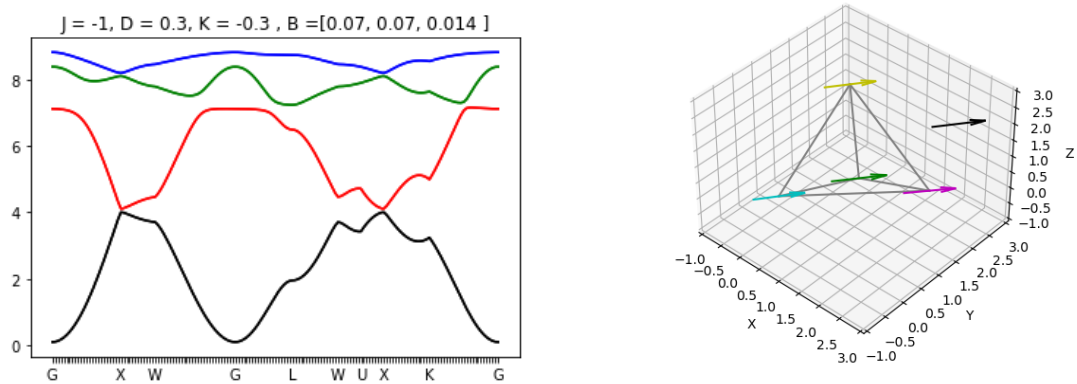


Figure 2.32:

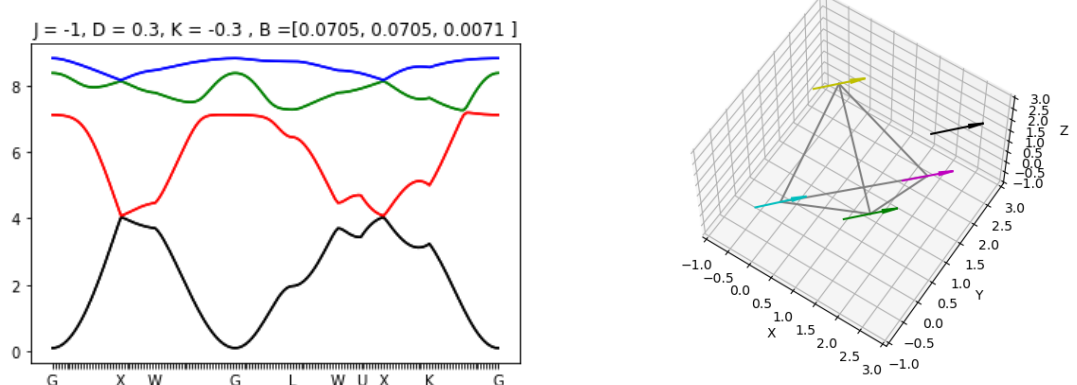


Figure 2.33:

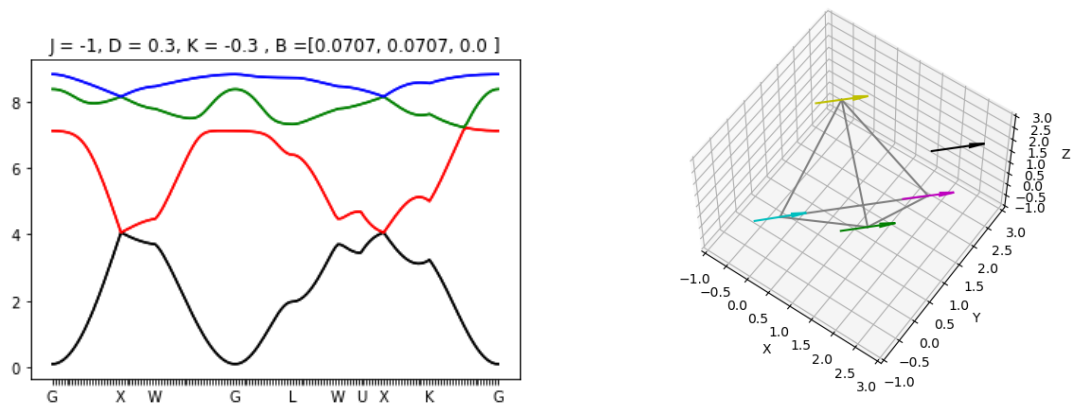


Figure 2.34:

# Chapter 3

## Summary and Conclusions

In presence of magnetic ferromagnetic splay state aligns with magnetic field direction. Magnon spectra change considerably compared to zero field case. Except for field along [100] direction, as the ground state already had a splay state along x. for [100] direction, degeneracy between X and W starts to lift. more interestingly, when field is along [111], bands separate completely, except for a single weyl point between band 2 and 3 on the path G and L. In all of these directions spectra has at least one weyl point and also at different positions. Hence by changing field direction we get weyl points at different positions for the pyrochlore system.

So far considerable amount of time has been spent on stabilizing the codes for our calculation. Now that we have the stability in the codes, our next motivation is to make the topological analysis of these magnon bands. We will then proceed to calculate the magnon spectrum of slab geometry of pyrochlore lattice in the presence of magnetic field. As most of the experimental results corresponds to slab geometries. where In bulk, we have the minimization task among 8 variables corresponding to 4 sub lattices. In slab geometry, if we have N layers in the truncated direction, we will have to do the minimization over 8N variables. This will be one of the main challenge in the slab geometry calculation.

As presented in Onose et al[8], Direction of field has no influence on thermal hall effect , Where as calculation by V.V Jyothis et. al.[3] for slab geometries show that , magnonic dispersion depends on direction of truncation for building the slabs. So, Magnon spectrum and Berry curvature calculation in slab geometries with presence of external field, will be the final goal as they are the two main ingredients to calculate thermal hall conductivity due to magnonic excitation and compare the results.

# Bibliography

- [1] Michael Victor Berry. “Quantal phase factors accompanying adiabatic changes”. In: *Proceedings of the Royal Society of London. A. Mathematical and Physical Sciences* 392.1802 (1984), pp. 45–57.
- [2] J.H.P. Colpa. “Diagonalization of the quadratic boson hamiltonian”. In: *Physica A: Statistical Mechanics and its Applications* 93.3 (1978), pp. 327–353. ISSN: 0378-4371. DOI: [https://doi.org/10.1016/0378-4371\(78\)90160-7](https://doi.org/10.1016/0378-4371(78)90160-7). URL: <https://www.sciencedirect.com/science/article/pii/0378437178901607>.
- [3] V. V. Jyothis, Bibhabasu Patra, and V. Ravi Chandra. *Magnon bands in pyrochlore slabs with Heisenberg exchange and anisotropies*. 2022. DOI: 10.48550/ARXIV.2210.03548. URL: <https://arxiv.org/abs/2210.03548>.
- [4] Hosho Katsura, Naoto Nagaosa, and Patrick A Lee. “Theory of the thermal Hall effect in quantum magnets”. In: *Physical review letters* 104.6 (2010), p. 066403.
- [5] JM Luttinger and L Tisza. “Theory of dipole interaction in crystals”. In: *Physical Review* 70.11-12 (1946), p. 954.
- [6] Alexander Mook, Jürgen Henk, and Ingrid Mertig. “Magnon Hall effect and topology in kagome lattices: A theoretical investigation”. In: *Physical Review B* 89.13 (2014), p. 134409.
- [7] Alexander Mook, Jürgen Henk, and Ingrid Mertig. “Tunable magnon Weyl points in ferromagnetic pyrochlores”. In: *Physical review letters* 117.15 (2016), p. 157204.
- [8] Y Onose et al. “Observation of the magnon Hall effect”. In: *Science* 329.5989 (2010), pp. 297–299.

# Appendix A

## A.1 Vanishing Linear terms in Local coordinates:

Let's write Spin components classically in local coordinates as

$$\begin{aligned} S_{i\alpha}^1 &= S \sin(\theta_{i\alpha}) \cos(\phi_{i\alpha}) \\ S_{i\alpha}^2 &= S \sin(\theta_{i\alpha}) \sin(\phi_{i\alpha}) \\ S_{i\alpha}^3 &= S \cos(\theta_{i\alpha}) \end{aligned} \quad (\text{A.1})$$

The ladder operator is:

$$\begin{aligned} S_{i\alpha}^\pm &= S \sin(\theta_{i\alpha}) e^{\pm i\phi_{i\alpha}} \\ H = & S^2 \sum_{i\alpha, j\beta} \left[ J_{i\alpha; j\beta}^{33} \cos(\theta_{i\alpha}) \cos(\theta_{j\beta}) + J_{i\alpha; j\beta}^{++} \sin(\theta_{i\alpha}) \sin(\theta_{j\beta}) e^{i\phi_{i\alpha}} e^{i\phi_{j\beta}} \right. \\ & + J_{i\alpha; j\beta}^{--} \sin(\theta_{i\alpha}) \sin(\theta_{j\beta}) e^{-i\phi_{i\alpha}} e^{-i\phi_{j\beta}} \\ & + J_{i\alpha; j\beta}^{+-} \sin(\theta_{i\alpha}) \sin(\theta_{j\beta}) e^{i\phi_{i\alpha}} e^{-i\phi_{j\beta}} \\ & + J_{i\alpha; j\beta}^{-+} \sin(\theta_{i\alpha}) \sin(\theta_{j\beta}) e^{-i\phi_{i\alpha}} e^{i\phi_{j\beta}} \\ & + J_{i\alpha; j\beta}^{+3} \sin(\theta_{i\alpha}) \cos(\theta_{j\beta}) e^{i\phi_{i\alpha}} + J_{i\alpha; j\beta}^{3+} \cos(\theta_{i\alpha}) \sin(\theta_{j\beta}) e^{i\phi_{j\beta}} \\ & \left. + J_{i\alpha; j\beta}^{-3} \sin(\theta_{i\alpha}) \cos(\theta_{j\beta}) e^{-i\phi_{i\alpha}} + J_{i\alpha; j\beta}^{3-} \cos(\theta_{i\alpha}) \sin(\theta_{j\beta}) e^{-i\phi_{j\beta}} \right] \\ & - S \sum_{i\alpha} \left[ \mathcal{B}_\alpha^3 \cos(\theta_{i\alpha}) + \mathcal{B}_\alpha^+ \sin(\theta_{i\alpha}) e^{i\phi_{i\alpha}} + \mathcal{B}_\alpha^- \sin(\theta_{i\alpha}) e^{-i\phi_{i\alpha}} \right] \end{aligned} \quad (\text{A.3})$$

Since the classical ground state configuration is the minimum of  $H$  We have:

$$\frac{\partial H}{\partial \theta_\alpha} \Big|_{\theta_\alpha=0, \phi_\alpha=\phi} = \frac{\partial H}{\partial \phi_\alpha} \Big|_{\theta_\alpha=0, \phi_\alpha=\phi} = 0; \quad \text{any } \phi \quad (\text{A.4})$$

By putting the  $\theta_\alpha = 0$  in  $\theta$  derivative of (A.3), we get

$$\sum_{j\beta} \left[ S \left( J_{i\alpha; j\beta}^{+3} + J_{j\beta; i\alpha}^{3+} \right) - B_\alpha^+ \right] e^{i\phi_\alpha} + \left[ S \left( J_{i\alpha; j\beta}^{-3} + J_{j\beta; i\alpha}^{3-} \right) - B_\alpha^- \right] e^{-i\phi_\alpha} = 0 \quad (\text{A.5})$$

This should be valid for every real  $\phi_\alpha$ , which means

$$S \sum_{j\beta} \left[ J_{i\alpha;j\beta}^{+3} + J_{j\beta;i\alpha}^{3+} \right] - B_\alpha^+ = 0; \quad \text{any } i\alpha \quad (\text{A.6})$$

$$S \sum_{j\beta} \left[ J_{i\alpha;j\beta}^{-3} + J_{j\beta;i\alpha}^{3-} \right] - B_\alpha^- = 0; \quad \text{any } i\alpha \quad (\text{A.7})$$

## A.2 High symmetry paths:

$$G = [0, 0, 0] X = [2\pi, 0, 0] W = [2\pi, \pi, 0] K = [3\pi/2, 3\pi/2, 0] L = [\pi, \pi, \pi] U = [2\pi, \pi/2, \pi/2]$$

$G$  is same as  $\Gamma$ .

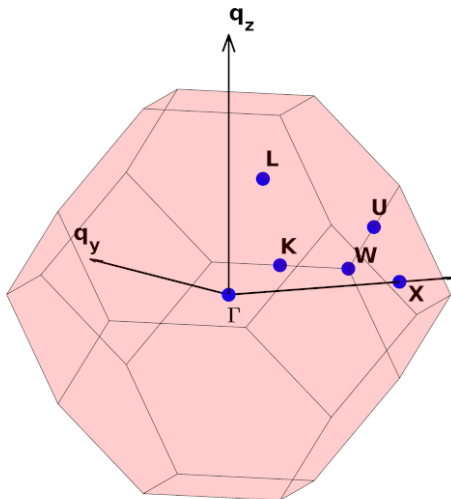


Figure A.1: Fcc Brillouin zone, For the high symmetry path listed before the figure.(figure imported from [3]) with permission

## A.3 Python Codes:

The python codes can be found at following github repository:

[https://github.com/airbendor890/9TH\\_semester\\_project\\_codes](https://github.com/airbendor890/9TH_semester_project_codes)